

Article

Properties of Carbonic Anhydrase-Containing Active Coatings for CO₂ Capture

Xiaobo Li ^{1,2,3}, Rui Zhou ², Haoran Yang ², Zimu Liang ², Yuxiang Yao ³, Zhipeng Yu ³, Mingsai Du ², Diming Lou ¹ and Ke Li ^{2,*}

¹ Automotive Department, Tongji University, Shanghai 200092, China; lixiaobo@smderi.com.cn (X.L.)

² Shanghai Marine Diesel Engine Research Institute, Shanghai 201108, China; zhourui@smderi.com.cn (R.Z.); yanghaoran@smderi.com.cn (H.Y.)

³ Shanghai Qiyao Environmentally Technology Co., Ltd., Shanghai 200082, China

* Correspondence: like@smderi.com.cn

Abstract: Carbonic anhydrase (CA)-based biological CO₂ capture is emerging as a prominent carbon capture and storage (CCS) technology. We developed a tagged CA-Ferritin chimera, resulting in a high-purity, high-activity, micrometer-sized CA aggregate, SazF, with a yield of 576.6 mg/L (protein/medium). SazF has an optimum temperature of 50 °C and demonstrates thermal stability between 40 and 60 °C. It operates efficiently in Tris-HCl buffer (pH = 8–9), making it compatible with ship exhaust conditions. For enhanced stability and reusability, SazF was encapsulated in SiO₂ and integrated into an epoxy resin to produce a corrosion-active coating. This coating, applied to foam metal fillers, showed less than 3% protein leakage after ten days and retained over 70% activity after a month at 60 °C. This simple preparation method and the cost-effective production of these biomaterials that can continuously and efficiently absorb CO₂ in high-temperature environments are suitable for most CO₂ capture devices. They have a broad application prospect in the field of industrial carbon capture.

Keywords: carbonic anhydrase; carbon capture; immobilization; stability



Citation: Li, X.; Zhou, R.; Yang, H.; Liang, Z.; Yao, Y.; Yu, Z.; Du, M.; Lou, D.; Li, K. Properties of Carbonic Anhydrase-Containing Active Coatings for CO₂ Capture. *Processes* **2024**, *12*, 810. <https://doi.org/10.3390/pr12040810>

Academic Editor: Davide Papurello

Received: 5 March 2024

Revised: 15 April 2024

Accepted: 15 April 2024

Published: 17 April 2024



Copyright: © 2024 by the authors. Licensee MDPI, Basel, Switzerland. This article is an open access article distributed under the terms and conditions of the Creative Commons Attribution (CC BY) license (<https://creativecommons.org/licenses/by/4.0/>).

1. Introduction

With the growth of the global shipping industry, carbon emissions from global shipping are increasing annually. Capturing carbon dioxide (CO₂) from ship exhaust is crucial for reducing CO₂ emissions and complying with strict emission regulations. Carbon capture and storage (CCS) technology is considered an effective method for reducing CO₂ emissions. Currently, carbon capture on ships commonly utilizes organic amine chemical absorption, which is divided into four parts: absorption, regeneration, compression, and liquefaction. This process has a large footprint and involves high energy consumption for solvent regeneration [1]. For instance, the regeneration of ethanolamine (MEA) solution constitutes approximately 60% of the total process energy consumption [2]. Therefore, it is necessary to find a green and low-energy CCS strategy that can replace the chemical absorption of organic amines.

Biological CO₂ capture technology, represented by carbonic anhydrase (CA, EC 4.2.1.1), has gradually become a research hotspot in CCS technology. CA, a stable, safe, and environmentally friendly biocatalyst, catalyzes the CO₂ hydration reaction, converting CO₂ into HCO₃[−] or CO₃^{2−} to efficiently capture flue gas CO₂ [3]. Several studies have been conducted to validate the feasibility of biologically based CO₂ capture technology. Leimbrink et al. [4] developed a biocatalyst delivery system (BDS) using immobilized CA active particulate material. This material was created by embedding CA in an organosilicon-based polymer matrix. Subsequently, the BDS system was tested in a small demonstration-scale CO₂ uptake performance in a countercurrent packed column. The results indicated that the total molar flux of CO₂ uptake increased by a factor of six in the presence of BDS

compared to the blank N-Methyldiethanolamine (MDEA) solvent. Gladis et al. [5] found that adding CA to the MDEA solvent had a positive impact on the CO₂ capture efficiency in uptake tests conducted on a pilot-packed column. Increasing the amount of enzyme added could enhance the capture efficiency. A 30% MDEA solvent can capture 18% to 23% of CO₂, and with the CA concentration increased to 3.5 g/L, the capture efficiency rises to 48% to 83% within the same range of liquid/gas ratio. The mass transfer performance of enzyme-enhanced solvents is approximately 80% of that of a 30 wt% MEA solvent solution.

In light of the facilitating impact of immobilization techniques on enzyme activity, stability, and reusability [6], it is crucial to identify a convenient and efficient immobilization technique to enable the industrial application of CA for CO₂ capture. Traditional immobilization methods include adsorption, cross-linking, covalent binding, encapsulation, entrapment, and cross-linked enzyme aggregates (CLEA) [7]. The first five methods rely on some form of interaction between the enzyme molecule and the carrier material to restrict the enzyme. In contrast, CLEA is a method of enzyme immobilization without using a carrier material [8].

Nanomaterials have been widely used for the immobilization of enzymes [9]. Nanosilica is a commonly used carrier for various catalysts because of its adjustable physicochemical properties, large specific surface area, high surface adsorption, and mechanical strength. It has been reported that CA was immobilized on silica particles. Hsieh et al. [10] demonstrated a 91% recovery of enzyme activity in the silylated form (R5-SazCA-SP) by fusing SazCA with an R5 peptide and biomineralizing it. R5-SazCA-SP exhibited twice as much residual activity as the free form after incubation for 35 days at 25 °C. Furthermore, R5-SazCA-SP retained 86% of its activity after 10 repetitions.

Meanwhile, the formation of oligomers of the target enzyme through the introduction of oligomerized peptides also contributes to enhancing the catalytic performance and stability of the recombinant enzyme [11,12]. Ferritin, a highly symmetric nanocage consisting of 24 subunits that can be spontaneously assembled [13–15], is a class of iron storage proteins that are widely found in plants and animals. Indeed, ferritin has special properties such as resistance to dilute acids (pH = 2.0), resistance to dilute bases (pH = 12.0), and resistance to higher temperatures (70–75 °C). Most of the ferritin nanocages remained resistant to incubation at 80 °C for 10 min. For example, the T_m value of human ferritin is about 82 °C [16,17]. Therefore, the structural and biochemical properties of ferritin could resist a high temperature and alkaline environment during CO₂ trapping.

In a previous study, we connected α -type CAs (SazCA) identified from the thermophilic bacterium *Sulfurihydrogenibium azorense* using a rigid linker to the oligomeric functional tag-ferritin and named the resulting complex SazCA-Ferritin (SazF). This approach enabled a cost-effective and efficient production of self-immobilized SazCA [18]. However, the challenge of separating the self-immobilized SazF powder from the absorbent solution may hinder the widespread application of carbonic anhydrases on a large scale. Therefore, in this study, to simplify the separation process, enhance enzyme stability, and enable the reuse of SazF, we incorporated SazF into chemically synthesized silica nanoparticles (SazF@SiO₂) using the sol-gel method. Additionally, we dispersed SazF@SiO₂ in epoxy resin coating to produce CA-active epoxy coatings. Furthermore, we characterized both the SazF@SiO₂ and the CA-containing coating. The SazF@SiO₂ and CA coatings were also characterized, and the stability and protein leakage rate of the coatings were tested.

2. Materials and Methods

2.1. Construction of Target Gene

The N-terminal of SazF is SazCA [19] (PBD ID: 4X5S), and the C-terminal is ferritin [20] (PDB ID: 2FHA); both are connected by a rigid linker, and the gene sequence of SazF was synthesized by GENEWIZ (GENEWIZ Biotechnology Co. Ltd., Suzhou, China). The target gene sequence was ligated to pET-22b(+) by double enzymatic cleavage and then introduced into the *Escherichia coli* BL21 (DE3) cell after being tested for accuracy by sequencing.

2.2. Expression and Purification of Recombinant Proteins

The 1% bacterial glycerol stock was cultured in Luria–Bertani (LB) medium containing one thousandth of ampicillin resistance at 37 °C, 200 r/min for 10 h, then inoculated into Terrific Broth (TB) medium according to the same bacterial ratio and cultured at 37 °C, 180 r/min, for 4 h of expanded culture; and we then added 1 mL 0.1 mol/L IPTG solution to make the final concentration of 0.5 mmol/L, 18 °C, 180 r/min, inducing culture for 20 h.

The precipitate obtained by centrifugation after culture was suspended in Tris–HCl buffer (25 mM, pH = 8.0). The cell suspension was ultrasonicated in an ice bath for 30 min (crushing power = 300 w) and then centrifuged at 4 °C, 3500× g at low speed for 10 min, and the target protein is insoluble precipitate.

The target protein is purified by low-speed centrifugation. The insoluble protein is re-suspended in Tris–HCl buffer, followed by centrifugation for 10 min at 3500× g, 4 °C; this is one round of purification, and 2 to 3 rounds of purification will result in a high purity of the target SazF. The purified SazF precipitate was frozen at –20 °C overnight (pre-frozen) and then put into a freeze dryer for 8 h to get SazF lyophilised powder.

2.3. Preparation of SazF@SiO₂ Particles

Tetramethoxysilane (TMOS) and hydroxyl-capped polydimethylsiloxane (PDMS-OH) in a molar ratio of 7.5:1 were added to the beaker. Subsequently, 0.5–1.0 g of 18-crown-6 was added, and the mixture was sonicated until it was completely dissolved. After that, 1.6 mL of Tris–HCl buffer (pH = 8.0) and 0.3–0.6 g of SazF freeze-dried powder were incorporated into the solution. To ensure uniform distribution, the mixture was stirred vigorously and then 80–100 µL of 1 M NH₄F solution was added to initiate the sol–gel reaction. Once a highly viscous gel material appeared at the bottom of the beaker, stirring was ceased. The resulting gel was subjected to drying overnight in an oven (55 °C) and subsequent freeze-drying 1 day, ultimately yielding SazF@SiO₂ particles embedded with CA.

2.4. Characterization of SazF@SiO₂ Particles

SEM test: Apreo 2C (Thermo Scientific, Waltham, MA, USA), energy spectrum Oxford ULTIM Max65 (Oxford Instruments, Abingdon, UK); TEM test: Thermo Fisher Scientific Talos F200S, Super X, 200 kV; BET test: Micromeritics ASAP 2460, sample degassing. Temperature: 120 degrees; XPS test conducted using the Thermo Fisher K-ALPHA instrument in the USA. The analysis chamber was under a vacuum of 8×10^{-10} Pa, with an excitation source of Al K α ray ($h\nu = 1486.6$ eV), operating at a voltage of 12.5 kV, filament current of 16 mA, and signal accumulation over 10 cycles.

2.5. Preparation of CA-Containing Coatings

A sample of 0.3–0.6 g of SazF@SiO₂ powder was accurately weighed and dispersed in Tris–HCl buffer (pH 8.0, 25 mmol/L) using ultrasonication. Subsequently, 2–5 mL of epoxy resin coating was added to the solution and stirred vigorously. The curing agent was then added while stirring, following a ratio of epoxy resin to curing agent of 4:1 by volume. After curing for 10 min, the resulting coating was uniformly applied to the pre-treated nickel foam filler (immersed in anhydrous ethanol and acetone for 30 min each). The nickel foam was then suspended in an oven at 55 °C for drying, ultimately resulting in the desired coating containing CA.

2.6. Esterase Activity

The reaction was set up by adding 100 mmol/L of acetonitrile-solubilized 4-Nitrophthalic acid (4-NPA) substrate to 1.8 mL of Tris–HCl buffer (25 mmol/L, pH = 8.0). Subsequently, 200 µL of a carbonic anhydrase solution at a certain concentration (the blank control included the addition of 200 µL of buffer) was added to the mixture. The absorbance at 348 nm was then measured after the reaction had occurred for 3 min at a specific temperature. For the immobilized carbonic anhydrase, a certain amount of SazF@SiO₂ was added to the solution, and the absorbance at 348 nm was again measured after the same reaction conditions. One

enzyme activity unit (IU) was defined as the amount of enzyme required to produce 1 μmol of p-nitrophenol (p-NP, p-Nitrophenol) per minute, and the specific activity was defined as the enzyme activity unit per mg of enzyme (IU/mg).

2.7. Optimum Temperature

The esterase activity of the recombinant protein was tested at various temperatures (30, 40, 50, 60, 70, 80, 90 °C) following the test method outlined in Section 2.5, with a recombinant protein amount of 0.425 mg. The highest activity was set at 100% to calculate the relative activity at other temperatures.

2.8. Thermal Stability

The recombinant protein or immobilized enzyme was incubated in a water bath at either 40, 50, or 60 °C. A portion of the enzyme solution or CA coating was taken for esterase activity testing every 2 h, following the procedures detailed in Section 2.6. The highest activity was set at 100%, and the remaining activities at different incubation times were calculated.

2.9. pH Stability

The recombinant protein solution was stored in Tris–HCl buffer at pH = 8.0 and 9.0 (pH = 8.0, 25 mmol/L), and a certain amount of the enzyme solution was taken at regular intervals for esterase activity testing; and the esterase activity testing method was the same as 2.5. The highest activity was set as 100%, and the remaining activities at different incubation times were calculated.

2.10. CO₂ Capture Capacity of SazF

The absorption of CO₂ by SazF at room temperature was evaluated through a bubbling experiment. A three-necked flask was charged with 10 mL of Tris–HCl buffer (pH = 9.0, 50 mM). SazF was then added to achieve a final concentration of 0.165 mg/mL. High-purity (99.9%) carbon dioxide was introduced into the flask at a rate of 0.8 L/min. The pH of the solution was periodically monitored, and the data were recorded until the solution stabilized. The control condition involved the use of Tris–HCl buffer without SazF.

2.11. Stability and Protein Leakage of CA-Containing Coatings

For the stability of the coatings containing CA, they were immersed in Tris–HCl buffer (pH = 8.0, 25 mmol/L) and incubated in a water bath at 60 °C for 30 days. The esterase activity was tested at intervals. The highest activity was set at 100%, and the remaining activities at different incubation times were calculated.

For the protein leakage assessment of the cellulose acetate (CA)-containing coatings, CA coatings were immersed in Tris–HCl buffer (pH = 8.0, 25 mmol/L) and stored at room temperature for 10 days. The protein content of the buffer was then tested at regular intervals. The protein content of the buffer was measured using the absorbance value at OD₂₈₀. The highest activity was on day 0, set at 100%. The protein leakage at different incubation times was calculated.

3. Results and Discussion

3.1. Expression and Purification of SazF

The composition and structure of SazF are shown schematically in Figure 1A,B. SazF was purified through three rounds of low-speed centrifugation. The results of SDS-PAGE electrophoresis are presented in Figure 1C, showing a distinct band near the molecular weight of 50 kDa, which closely matched the theoretically calculated value of 51 kDa for SazF. In addition, recombinant SazF can be purified through low-speed centrifugation without the need for complex and costly chromatographic purification. Histidine-tag purification methods are complex, expensive, and challenging to scale up. It was previously reported that the typical yield of protein product purified using His-tag without tag removal

and pMAL fusion with tag removal was 74 mg/L and 40 mg/L, respectively. In contrast, the yield of SazF in this paper was 576.6 mg/L, which was approximately 7.79 and 14.42 times higher than that of the first two methods [21]. This lays the foundation for the large-scale preparation of carbonic anhydrase. Indeed, the total cost per kilogram of protein product purified using the first two methods was \$838,124.73 and \$9,664,682.82, respectively, while the cost with the ferritin tag was \$52,810, which accounted for only 6.30% and 0.55% of the cost of the first two methods. What is more, the cost of preparing SazF accounts for only 1.89% of the selling price of commercial carbonic anhydrase (e.g., \$3806 for commercial carbonic anhydrase per gram). The above results indicate that the target protein SazF was successfully expressed and purified with a high yield of the target protein at a low purification cost, making it suitable for large-scale preparation and industrial applications.

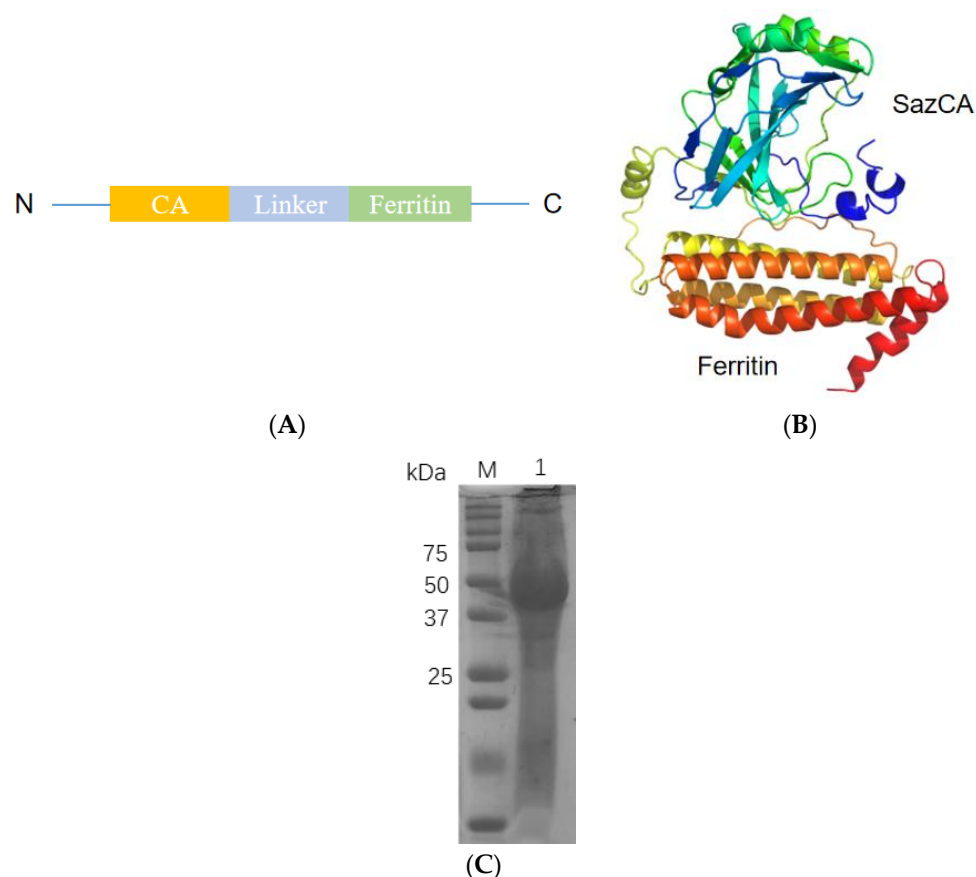


Figure 1. Recombinant protein of SazF. (A) Schematic representation of the recombinant expression plasmid pET-SazCA-Ferritin; (B) Schematic diagram of the structure of SazCA+ linker + Ferritin; (C) SDS-PAGE analysis of SazF protein—Lane M: Marker; Lane 1: Purified SazF.

Indeed, we also discovered a very interesting phenomenon: the insoluble form of SazF can spontaneously dissolve into a smaller, soluble form at room temperature. SazF is an active protein precipitate that is similar in nature to active inclusion bodies. Unlike inclusion bodies, which require high concentrations of urea for re-solubilization, SazF forms aggregates of nanoscale particles that partially dissolve in buffer. This process ultimately leads to an equilibrium between micrometer- and nanoscale SazF in the buffer. The transmission electron microscopy (TEM) testing showed that its size had transformed from the micrometer to nanometer scale. As shown in Figure 2A, the TEM results indicate that the insoluble SazF has an ellipsoidal morphology with an average particle size of approximately 1.0 μm , whereas the soluble SazF assumes a spherical morphology with a size of approximately 10 nm. It is worth emphasizing that this study primarily focuses on the insoluble form of SazF.

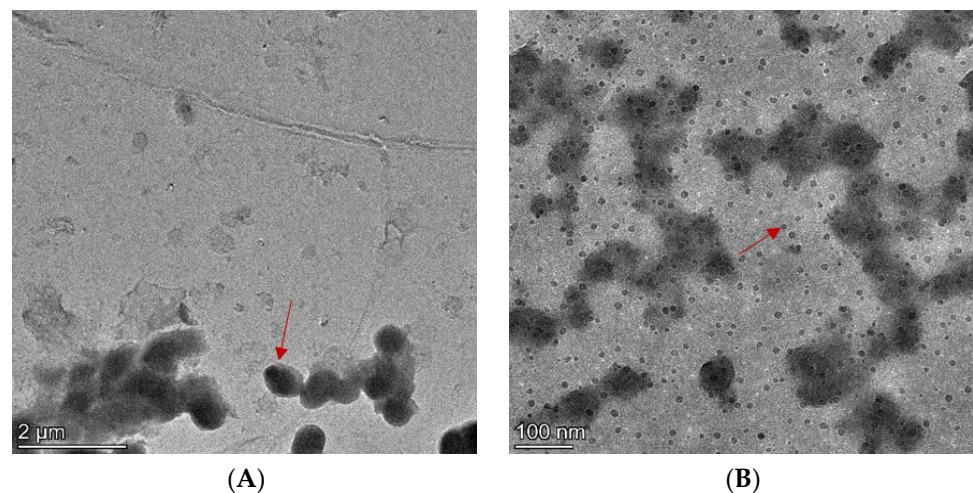


Figure 2. TEM results of insoluble and soluble SazF. **(A)** Insoluble SazF; **(B)** Soluble SazF. Red arrows point to micrometer-scale carbonic anhydrase aggregates **(A)** and dispersed nanoscale carbonic anhydrase **(B)**, respectively.

3.2. Optimum Temperature of Recombinant Proteins

As shown in Figure 3, the relative specific activity of SazF exhibited an overall trend of increasing and then decreasing with the rise in temperature, reaching its peak at 50 °C, which is the optimal temperature for SazF. In addition, the increase in temperature did not have a particularly large effect on the specific activity. The specific activity of SazF at 60 °C was 91.2% of that at the optimal temperature. At 70 °C, the specific activity of SazF was 83.9% of the optimal temperature. It is noteworthy that even when the temperature reached 90 °C, the specific activity of SazF was still able to reach 60.9% of the optimal temperature. It should be emphasized that when the temperature reached 90 °C, the specific activity of SazF still reached 60.9% of the optimal temperature. This indicates that SazF can tolerate high temperatures for a short period of time. Other researchers have also tested the optimal temperature of carbonic anhydrase and achieved desirable results. For example, Ki et al. [22] cloned a novel *Hahella chejuensis* α -CA (HC-aCA) with an optimal temperature of 50 °C. Jun et al. [23] cloned a novel CA from the Gram-negative marine bacterium *Alivibrio salmonicida*, subjected it to codon optimization, and excised the signal peptide. The obtained mASCA can be stable in the range of 10–60 °C, with its optimum temperature being 40 °C.

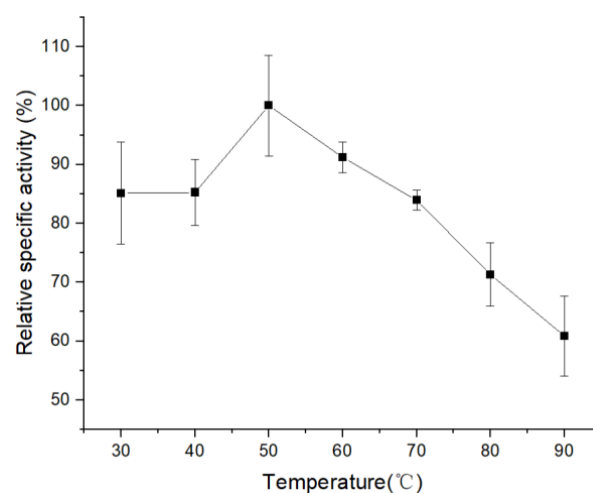


Figure 3. Optimum temperature of recombinant proteins.

3.3. Temperature and pH Stability of Recombinant Proteins

Since the temperature of ship exhaust after cooling ranges between 40 and 60 °C [24], and since the absorbent tends to be an alkaline solution [25], we conducted tests to assess the thermal stability of the recombinant protein at 40, 50, and 60 °C, as well as its stability at pH levels of 8 and 9. The temperature stability is shown in Figure 4A. The recombinant protein exhibits the highest activity at 60 °C, followed by 50 °C and 40 °C. The activity trend at this temperature is correct because the optimum temperature for free SazCA is 80 °C [26]. The recombinant protein is thermally stable at 40–60 °C, and the relative activity values after incubation for 12 h all increased compared to the initial activity values. This increase may be attributed to the insoluble recombinant protein partially converting to soluble nano-enzymes during the incubation process, thereby enhancing the activity. Other researchers have also found excellent thermal stability in some carbonic anhydrase enzymes. For instance, Byung et al. [27] discovered that TaCA from *Thermovibrio ammonificans* exhibited thermal stability with a half-life of 77 days at 60 °C. Additionally, Ricardo et al. [28] obtained the N140G carbonic anhydrase mutant through rational design, which had a half-life of 271 days.

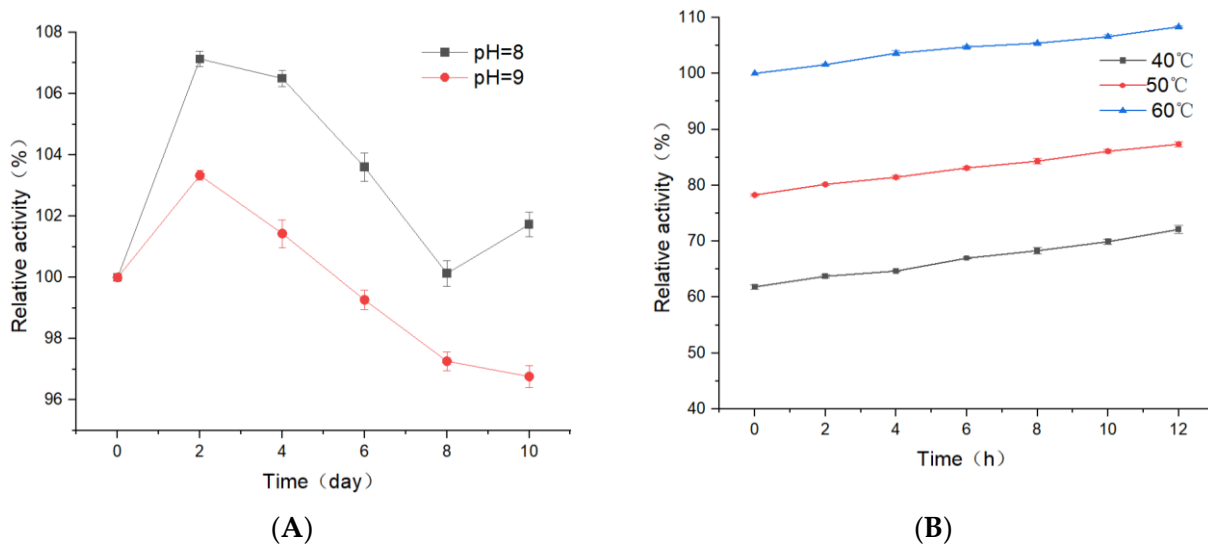


Figure 4. Stability of recombinant proteins. (A) pH stability; (B) Temperature stability.

The pH stability is illustrated in Figure 4B. The relative activity values initially increased and then decreased. The increase in activity values was attributed to the partial solubilization of insoluble recombinant proteins. After 2 days of incubation, the relative activity values began to decrease. However, after 10 days of incubation, the relative activity values were 101.7% and 96.8% at pH 8 and pH 9, respectively. This indicates its ability to withstand alkaline conditions. This finding is consistent with the research by Heuer et al. [29] and aligns with the characteristic of CA being more active in alkaline environments [30]. Other researchers have also found excellent pH stability of some carbonic anhydrase enzymes. For instance, Faridi et al. [31] isolated a dimeric α -CA from the alkaliphilic, moderately thermophilic, and halotolerant *Bacillus halodurans* TSLV1, naming it BhCA. This enzyme can maintain stability within the pH range of 6.0–11.0.

3.4. CO₂ Capture Capacity of SazF

The pH changes during CO₂ absorption in the Tris–HCl buffer (pH = 9.0, 50 mM) at room temperature, both in the presence and absence of SazF, are displayed in Figure 5. In the blank control (absence of SazF), the initial pH was 9.17, which decreased to 6.4 after 6 min of reaction. Furthermore, the pH of the buffer containing SazF, initially at 9.24, dropped to 6.33 after the reaction. While the pH differences (Δ pH) between the two conditions were similar, the presence of SazF significantly accelerated the rate of pH

change. At 60 s, the pH of the blank control had decreased to 8.0, whereas the pH of the experimental group had already dropped to 6.59. These findings suggest that SazF effectively enhances CO₂ absorption by the buffer.

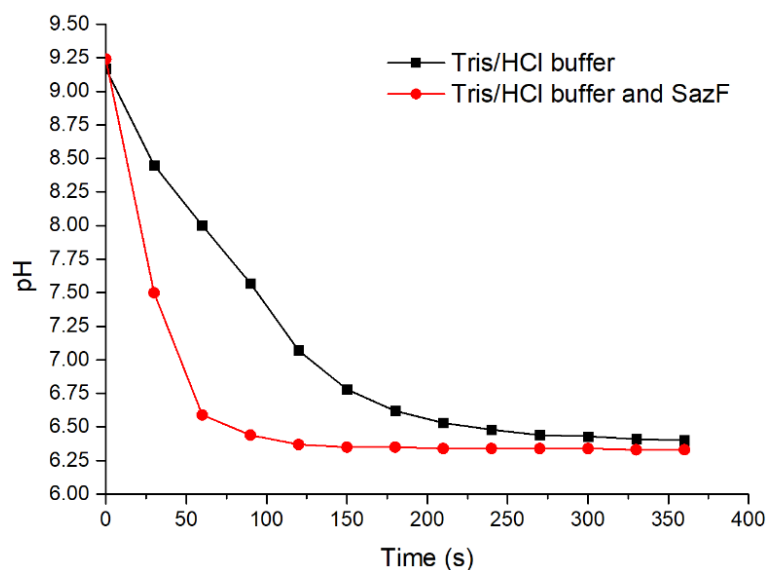


Figure 5. CO₂ hydration catalyzed by recombinant CAs.

3.5. Characterization of SazF@SiO₂ Particles

The SEM and TEM tests conducted on the SazF@SiO₂ particles, as displayed in Figure 6A,B, revealed the formation of micron-sized aggregates with rough surfaces due to the aggregation of numerous nanostructures. The aggregates measured approximately 5–15 μm in size. Furthermore, the EDS analysis, as shown in Figure 6B, indicated the presence of N, O, Si, and Zn elements in the gel particles. The XPS results, presented in Figure 6C,D, further supported the presence of these elements within the particles. Given that carbonic anhydrase is a Zn-containing metalloenzyme, these characterization outcomes confirmed the synthesis of SiO₂ and the successful encapsulation of carbonic anhydrase within the SazF@SiO₂ particles.

The BET results of SazF@SiO₂ particles are shown in Table 1. The specific surface area of the material is 0.2032 m²/g; the pore volume is 0.003246 cm³/g; and the pore size is 63.8903 nm. What is more, the CA loading in the particles is 8.3%, and the specific viability of the particles was 1.22 U/mg. The pore size of the particles is closely related to the amount of carbonic anhydrase immobilized. The larger the pore size, the better the pore penetration, resulting in higher immobilized particle activity. Moreover, the larger the specific surface area of nanomaterials, the more active sites per unit mass of catalysts are exposed, and the more favorable for catalytic activity, the greater the contact between the particles and the substrate, which is more conducive to the particles' carbon capture. For example, Shao et al. [32] immobilized CA on different silica-based mesoporous molecular sieves, and the average pore sizes of the particles with carbonic anhydrase immobilized on SBA-15/CA, KIT-6/CA, and MCM-41/CA were 9.6, 4.9, and 2.8 nm, while the specific surface areas were 420, 545, and 854 m²/g, respectively. The enzyme loadings on KIT-6, SBA-15, and MCM-41 were about 4.7, 6.1, and 5.2%, respectively. The relative activities were 36%, 78%, and 82% for each material, respectively. The particles prepared in this study had a low specific surface area and were macroporous. Therefore, further optimization processes are needed to improve the catalytic activity in future studies.

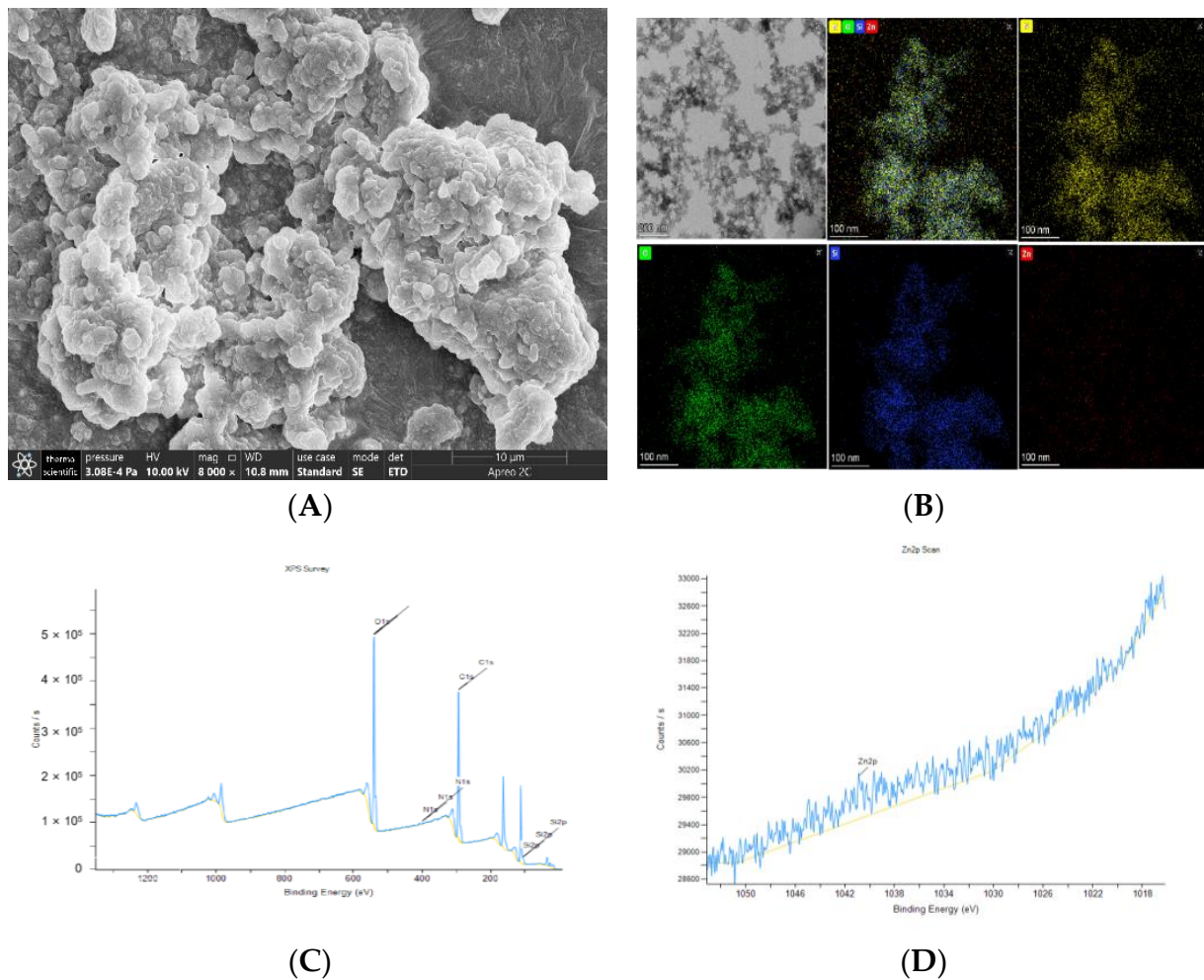


Figure 6. SazF@SiO₂ particle characterization results. (A) SEM results; (B) TEM and EDS results (the different colors represent the different elements present in the gel particles: yellow for nitrogen, green for oxygen, blue-violet for silicon, and red for zinc); (C,D) XPS analysis.

Table 1. BET characterization data of SazF@SiO₂ particles.

BET Surface Area	Pore Volume	Pore Size
0.2032 m ² /g	0.003246 cm ³ /g	63.8903 nm

3.6. Characterization of CA-Containing Coatings

SEM characterization of the coatings containing CA was performed. As depicted in Figure 7A, the left side displays nickel foam metal coated with gel particles, while the right side shows nickel foam metal without coating (control). Figure 7B illustrates nickel foam metal without carbonic anhydrase coating, presenting a smooth surface. In contrast, Figure 7C exhibits nickel foam metal with carbonic anhydrase coating, showcasing a rough surface, indicating the successful coating of CA on the foam metal. In addition, the esterase activity of the CA-containing coating was 16.02 U.

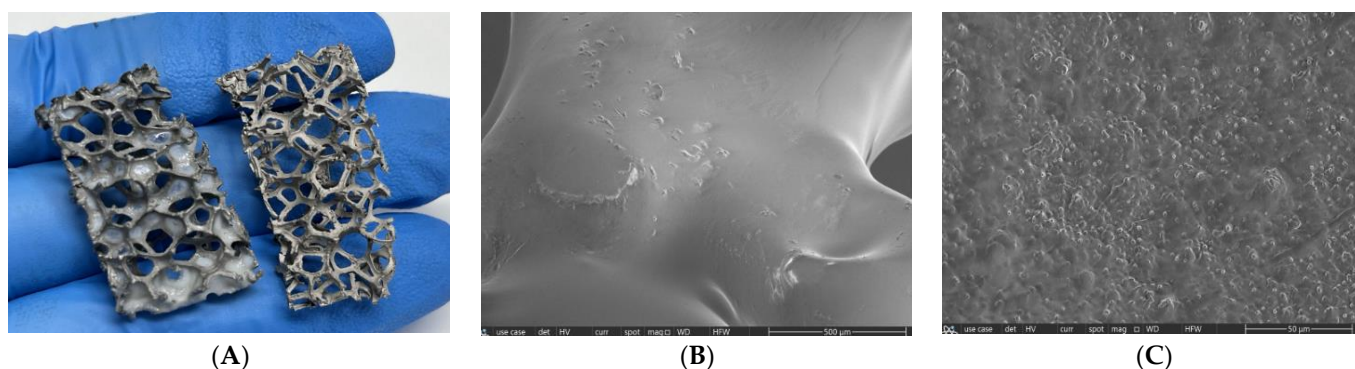


Figure 7. Characterization results of CA-containing coatings. (A) Coating of the foam metal filler: the left side shows the foam metal filler with CA coating, and the right side shows the uncoated foam metal filler; (B,C) show the SEM results of the foam metal filler before and after coating: where (B) is the uncoated foam metal filler, and (C) the foam metal filler after coating.

3.7. Thermal Stability and Protein Leakage Rate of CA-Containing Coatings

To evaluate the carbon trapping performance of the CA-containing coating, the stability of the coating at 60 °C and the protein leakage rate of the coating at room temperature for 10 days were tested. The results are shown in Figure 8A, indicating that the thermal stability of the coating was good. The residual activity was about 90% of the initial activity after 10 days of incubation at 60 °C. After 30 days of incubation, the residual activity was about 70% of the initial activity. Other researchers have also found that immobilization improves the thermal stability of carbonic anhydrase. For example, Ying et al. [33] prepared a core-shell magnetic ZIF-8@Fe₃O₄-carbonic anhydrase biocatalyst and tested its thermal stability at 40 °C, which showed that the residual activity of the immobilized enzyme was about 30% higher than that of the free enzyme after 9 days of incubation. In addition, as shown in Figure 8B, the coating showed less than 3% protein leakage after 10 days at room temperature, suggesting that the coating was able to firmly encapsulate the SazF@SiO₂ particles. Cristhian et al. [34] immobilized the carbonic anhydrase enzyme in a poly-particulate liquid, and the immobilized enzyme showed good stability during storage, with no loss of activity detected after 1 month. The above results indicate that the coating is stable and can consistently and efficiently capture CO₂ over an extended period.

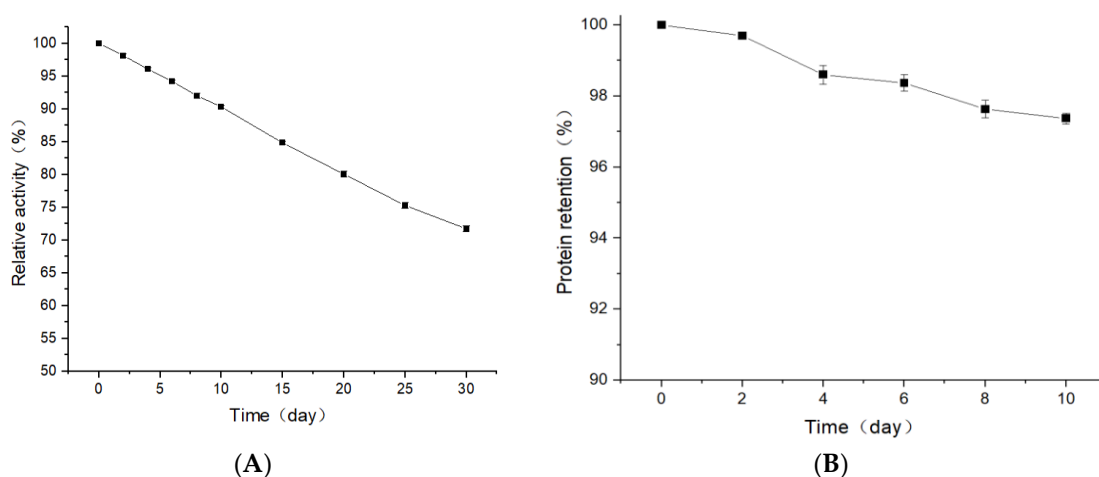


Figure 8. Stability of CA-containing coatings. (A) Stability of CA-containing coatings at 60 °C; (B) Protein leakage rate of CA-containing coatings.

4. Conclusions

In order to prepare biocatalysts suitable for carbon capture on ships, we constructed SazCA and ferritin chimeras (SazF). The preparation cost of SazF was approximately 1.89% of that of the commercial enzyme, significantly reducing the overall preparation cost of the biocatalysts. The incorporation of ferritin made SazF thermally stable and resistant to alkaline conditions within the range of 40–60 °C. Furthermore, SazF effectively enhances CO₂ absorption by the buffer. To facilitate the reuse of SazF, it is embedded in SiO₂ particles (SazF@SiO₂), with the CA loading in the particles being 8.3%. In order to reduce the separation cost, SazF@SiO₂ was integrated into an epoxy resin to produce a CA-active coating, which was stable at 60 °C and had good storage stability. This research aims to facilitate the application of biocatalysts for carbon capture on ships. Follow-up studies will further investigate the influencing factors of the fixation and coating processes, the effects of the type of absorbent used for SazF, the composition of ship exhaust, and the process parameters of the experimental bench absorption process on the absorption of CO₂ by carbonic anhydrase. Additionally, we aim to explore the operational stability of SazF in bench experiments and evaluate the effectiveness of the absorption on the bench as well as the cost of the process.

Author Contributions: Conceptualization and methodology, X.L.; writing—original draft preparation, R.Z.; formal analysis, H.Y.; visualization, Z.L.; investigation, Y.Y.; resources, Z.Y.; data curation, M.D.; supervision, D.L.; writing—review and editing, K.L. All authors have read and agreed to the published version of the manuscript.

Funding: This research was funded by the project entitled “National Key R&D Program of China”, Project no. 2022YFE0124300 and 2022YFE0208900.

Data Availability Statement: Data are contained within the article.

Conflicts of Interest: Authors Xiaobo Li, Yuxiang Yao and Zhipeng Yu were employed by the company Shanghai Qiyao Environmentally Technology Co., Ltd. The remaining authors declare that the research was conducted in the absence of any commercial or financial relationships that could be construed as a potential conflict of interest. The Shanghai Qiyao Environmentally Technology Co., Ltd. had no role in the design of the study; in the collection, analyses, or interpretation of data; in the writing of the manuscript, or in the decision to publish the results.

Abbreviations

CA	carbonic anhydrase
CCS	carbon capture and storage
CO ₂	carbon dioxide
4-NPA	4-Nitrophthalic acid
BDS	biocatalyst delivery system
MEA	ethanolamine
MDEA	N-Methyldiethanolamine
CLEA	cross-linked enzyme aggregates
LB	Luria–Bertani
TB	Terrific Broth
TMOS	tetramethoxysilane
PDMS-OH	hydroxyl-capped polydimethylsiloxane
SazF	SazCA-Ferritin

References

- Hua, W.S.; Sha, Y.S.; Zhang, X.L.; Cao, H. Research progress of carbon capture and storage (CCS) technology based on the shipping industry. *Ocean Eng.* **2023**, *281*, 114929. [[CrossRef](#)]
- Liu, S.; Gao, H.X.; He, C.; Liang, Z.W. Experimental evaluation of highly efficient primary and secondary amines with lower energy by a novel method for post-combustion CO₂ Capture. *Appl. Energy* **2019**, *233–234*, 443–452. [[CrossRef](#)]
- Smith, K.S.; Ferry, J.G. Prokaryotic carbonic anhydrases. *FEMS Microbiol. Rev.* **2000**, *24*, 335–366. [[CrossRef](#)] [[PubMed](#)]

4. Leimbrink, M.; Nikoleit, K.G.; Spitzer, R.; Salmon, S.; Buchholz, T.; Górak, A.; Skiborowski, M. Enzymatic reactive absorption of CO₂ in MDEA by means of an innovative biocatalyst delivery system. *Chem. Eng. J.* **2018**, *334*, 1195–1205. [[CrossRef](#)]
5. Gladis, A.; Lomholdt, N.F.; Fosbøl, P.L.; Woodley, J.M.; Solms, N.V. Pilot scale absorption experiments with carbonic anhydrase-enhanced MDEA- Benchmarking with 30 wt% MEA. *Int. J. Greenh. Gas Control* **2019**, *82*, 69–85. [[CrossRef](#)]
6. Mateo, C.; Palomo, J.M.; Fernandez-Lorente, J.; Jose, M.G.; Fernandez-Lafuente, R. Improvement of enzyme activity, stability and selectivity via immobilization techniques. *Enzym. Microb. Technol.* **2007**, *40*, 1451–1463. [[CrossRef](#)]
7. Sánchez-deAlcázar, D.; Liutkus, M.; Cortajarena, A.L. Immobilization of enzymes in protein films. *Methods Mol. Biol.* **2020**, *2100*, 211–226. [[PubMed](#)]
8. Cao, L.; Langen, L.V.; Sheldon, R.A. Immobilised enzymes: Carrier-bound or carrier-free? *Curr. Opin. Biotechnol.* **2003**, *14*, 387–394. [[CrossRef](#)] [[PubMed](#)]
9. Sharifi, M.; Robotjazi, S.M.; Sadri, M.; Mosaabadi, J.M. Covalent immobilization of organophosphorus hydrolase enzyme on chemically modified cellulose microfibers: Statistical optimization and characterization. *Polymers* **2018**, *124*, 162–170. [[CrossRef](#)]
10. Hsieh, C.J.; Cheng, J.C.; Hu, C.J.; Yu, C.Y. Entrapment of the fastest known carbonic anhydrase with biomimetic silica and its application for CO₂ sequestration. *Polymers* **2021**, *13*, 2452. [[CrossRef](#)]
11. Zhang, L.; Lei, L.C.; Zhang, G.Y.; Li, X.L. Oligomerization triggered by foldon to enhance the catalytic efficiency of feruloyl esterase. *Chin. J. Biotechnol.* **2019**, *35*, 816–826.
12. Wang, X.Z.; Ge, H.H.; Zhang, D.D.; Wu, S.Y.; Zhang, G.Y. Oligomerization triggered by foldon: A simple method to enhance the catalytic efficiency of lichenase and xylanase. *BMC Biotechnol.* **2017**, *17*, 57. [[CrossRef](#)] [[PubMed](#)]
13. Zhang, J.L.; Chen, X.H.; Hong, J.J.; Tang, A.; Liu, Y.; Xie, N.; Nie, G.; Yan, X.; Liang, M. Biochemistry of mammalian ferritins in the regulation of cellular iron homeostasis and oxidative responses. *Sci. China Life Sci.* **2021**, *64*, 352–362. [[CrossRef](#)]
14. Yao, H.; Soldano, A.; Fontenot, L.; Donnarumma, F.; Lovell, S.; Chandler, J.R.; Rivera, M. *Pseudomonas aeruginosa* bacterioferritin is assembled from FtnA and BfrB subunits with the relative proportions dependent on the environmental oxygen availability. *Biomolecules* **2022**, *12*, 366. [[CrossRef](#)]
15. Honarmand Ebrahimi, K.; Hagedoorn, P.L.; Hagen, W.R. Unity in the biochemistry of the iron-storage proteins ferritin and bacterioferritin. *Chem. Rev.* **2015**, *115*, 295–326. [[CrossRef](#)]
16. Chen, H.; Tan, X.; Han, X.; Ma, L.; Dai, H.; Fu, Y.; Zhang, Y. Ferritin nanocage based delivery vehicles: From single- to compartmentalized-encapsulation of bioactive or nutraceutical compounds. *Biotechnol. Adv.* **2022**, *61*, 108037. [[CrossRef](#)]
17. Li, H.; Tan, X.; Xia, X.; Zang, J.; El-Seedi, H.; Wang, Z.; Du, M. Improvement of thermal stability of oyster (*Crassostrea gigas*) ferritin by point mutation. *Food Chem.* **2021**, *346*, 128879. [[CrossRef](#)]
18. Mao, L.; Liu, G.Z.; Yuan, H.; Zhang, G.Y. Efficient preparation of carbon anhydrase nanoparticles capable of capturing CO₂ and their characteristics. *Chem. Eng. J.* **2023**, *74*, 2589–2598.
19. De Simone, G.; Monti, S.M.; Alterio, V.; Buonanno, M.; De Luca, V.; Rossi, M.; Carginale, V.; Supuran, C.T.; Capasso, C.; Di Fiore, A. Crystal structure of the most catalytically effective carbonic anhydrase enzyme known, SazCA from the thermophilic bacterium *Sulphurihydrogenibium azorense*. *Bioorg. Med. Chem. Lett.* **2015**, *25*, 2002–2006. [[CrossRef](#)]
20. Hempstead, P.D.; Yewdall, S.J.; Fernie, A.R.; Lawson, D.M.; Artymiuk, P.J.; Rice, D.W.; Ford, G.C.; Harrison, P.M. Comparison of the three-dimensional structures of recombinant human H and horse L ferritins at high resolution. *J. Mol. Biol.* **1997**, *268*, 424–448. [[CrossRef](#)]
21. Banki, M.R.; Wood, D.W. Inteins and affinity resin substitutes for protein purification and scale up. *Microb. Cell Fact.* **2005**, *4*, 32. [[CrossRef](#)] [[PubMed](#)]
22. Ki, M.R.; Min, K.; Kanth, B.K.; Lee, J.; Pack, S.P. Expression, reconstruction and characterization of codon-optimized carbonic anhydrase from *Hahella chejuensis* for CO₂ sequestration application. *Bioprocess Biosyst. Eng.* **2013**, *36*, 375–381. [[CrossRef](#)] [[PubMed](#)]
23. Jun, S.Y.; Kim, S.H.; Kanth, B.K.; Lee, J.; Pack, S.P. Expression and characterization of a codon-optimized alkaline-stable carbonic anhydrase from *Aliivibrio salmonicida* for CO₂ sequestration applications. *Bioprocess Biosyst. Eng.* **2017**, *40*, 413–421. [[CrossRef](#)]
24. Liu, X.; Zhao, C.; Guo, H.; Wang, Z. Performance Analysis of Ship Exhaust Gas Temperature Differential Power Generation. *Energies* **2022**, *15*, 3900. [[CrossRef](#)]
25. Melnikov, S.M.; Stein, M. The effect of CO₂ loading on alkanolamine absorbents in aqueous solutions. *Phys. Chem. Chem. Phys.* **2019**, *21*, 18386–18392. [[CrossRef](#)]
26. Luca, V.D.; Vullo, D.; Scozzafava, A.; Carginale, V.; Rossi, M.; Supuran, C.T.; Capasso, C. An α -carbonic anhydrase from the thermophilic bacterium *Sulphurihydrogenibium azorense* is the fastest enzyme known for the CO₂ hydration reaction. *Bioorg. Med. Chem.* **2013**, *21*, 1465–1469. [[CrossRef](#)]
27. Jo, B.H.; Seo, J.H.; Cha, H.J. Bacterial extreme- α -carbonic anhydrases from deep-sea hydrothermal vents as potential biocatalysts for CO₂ sequestration. *J. Mol. Catal. B Enzym.* **2014**, *109*, 31–39. [[CrossRef](#)]
28. Parra-Cruz, R.; Jäger, C.M.; Lau, P.L.; Gomes, R.L.; Pordea, A. Engineering of *Thermovibrio ammonificans* carbonic anhydrase mutants with increased thermostability. *J. CO₂ Util.* **2020**, *37*, 1–8. [[CrossRef](#)]
29. Heuer, J.; Kraus, Y.; Vučak, M.; Zeng, A.P. Enhanced sequestration of carbon dioxide into calcium carbonate using pressure and a carbonic anhydrase from alkaliphilic *Coleofasciculus chthonoplastes*. *Eng. Life Sci.* **2021**, *22*, 178–191. [[CrossRef](#)]
30. Zhu, Y.; Liu, Y.; Ai, M.; Jia, X. Surface display of carbonic anhydrase on *Escherichia coli* for CO₂ capture and mineralization. *Synth. Syst. Biotechnol.* **2022**, *7*, 460–473. [[CrossRef](#)]

31. Faridi, S.; Satyanarayana, T. Novel alkalistable α -carbonic anhydrase from the polyextremophilic bacterium *Bacillus halodurans*: Characteristics and applicability in flue gas CO₂ sequestration. *Environ. Sci. Pollut. Res.* **2016**, *23*, 15236–15249. [[CrossRef](#)] [[PubMed](#)]
32. Shao, P.J.; Chen, H.; Ying, Q.; Zhang, S.H. Structure–Activity relationship of carbonic anhydrase enzyme immobilized on various silica-based mesoporous molecular sieves for CO₂ absorption into a potassium carbonate solution. *Energy Fuels* **2020**, *34*, 2089–2096. [[CrossRef](#)]
33. Ying, Q.; Chen, H.; Shao, P.; Zhou, X.; He, X.; Ye, J.; Zhang, S.; Chen, J.; Wang, L. Core-shell magnetic ZIF-8@Fe₃O₄-carbonic anhydrase biocatalyst for promoting CO₂ absorption into MDEA solution. *J. CO₂ Util.* **2021**, *49*, 101565. [[CrossRef](#)]
34. Molina-Fernandez, C.; Peters, A.P.; Debecker, D.P.; Luis, P. Immobilization of carbonic anhydrase in a hydrophobic poly (ionic liquid): A new functional solid for CO₂ capture. *Biochem. Eng. J.* **2022**, *187*, 108639. [[CrossRef](#)]

Disclaimer/Publisher’s Note: The statements, opinions and data contained in all publications are solely those of the individual author(s) and contributor(s) and not of MDPI and/or the editor(s). MDPI and/or the editor(s) disclaim responsibility for any injury to people or property resulting from any ideas, methods, instructions or products referred to in the content.